基于谱位移格式的复杂切口功能梯度板自由振动等几何分析

杨少伟[1],孙贤波[1],蔡志勤[1*],卢海龙[1],杨志勋[2]

1. 大连理工大学工程力学系,大连 116024
2. 哈尔滨工程大学机电工程学院,哈尔滨 150001

摘要 为分析具有复杂切口的功能梯度板自由振动响应,基于一种新的准三维高阶剪切变形理论(谱位移格式)的等几何分析方法被用来预测带切口板的动力特性。谱位移格式将未知位移场展开为厚度方向上特殊形式的切比雪夫级数,具有精度高,以及避免剪切闭锁问题的特性,对薄厚板的分析具有很好的通用性。利用达朗贝尔原理和虚功原理推导了功能梯度板自由振动的控制方程,并利用等几何方法对方程进行离散和求解。通过对数值算例的计算,以及与现有参考结果的比较,证明了提出的分析方法能够准确有效地分析具有复杂切口的功能梯度板自由振动问题。

关键词 功能梯度板;复杂切口;谱位移格式;等几何分析;自由振动

功能梯度材料是一种多相材料,具有成分和材料性能随体积变化而变化的特性[1]。功能梯度板具有高刚度、高强度、轻质量,以及耐磨性好、隔热性强等特点,在海洋工程业、船舶业、航空航天业、建筑业和医疗设备等众多领域得到广泛应用[2]。在实际应用中,例如,在船舶和海洋结构中,为了减轻质量或者应对通风、检查、机械连接等需求,通常在功能梯度板上引入复杂切口[3]。切口的存在会改变结构整体或部分的力学性能,从而导致动态稳定性的丧失。因此,为了结构的有效设计和安全,对复杂切口的功能梯度板进行动力学分析是十分必要的。

在机械或热载荷作用下,简单边界条件下无切口板响应的封闭形式解很容易获得。然而,当在板上开孔后,切孔引入新的无牵引力边界,导致解析解很难获得,需要各种数值、实验方法来分析这种有切口板。相应的数值方法包括有限元法[4]、有限

收稿日期:2023-06-02;修回日期:2023-07-09
基金项目:国家自然科学基金项目(52271269,52001088,U2241263,U1906233)
作者简介:杨少伟,博士研究生,研究方向为等几何分析,电子信箱:qinchao98998@mail.dlut.edu.cn;蔡志勤(通信作者),教授,研究方向为动力学与控制,电子信箱:zhqcai@dlut.edu.cn
引用格式:杨少伟, 孙贤波, 蔡志勤, 等. 基于谱位移格式的复杂切口功能梯度板自由振动等几何分析[J]. 科技导报, 2024, 42(13): 36-47;
doi: 10.3981/j.issn.1000-7857.2023.09.01364

样条法[5]、扩展有限元法[6]、广义微分正交有限元法[7]、变分微分正交法[8]、无网格法[9]和等几何分析[10]。其中,等几何分析(IGA)是一种新颖的数值方法[11],它可以实现几何建模和数值模拟的无缝衔接。能够精确地描述复杂切口形状,减小数值误差,同时还可以轻易地满足任意阶连续性要求,在板壳等结构单元的构造上优势明显。

用于功能梯度板振动分析的剪切变形理论可分经典板理论(CPT)、一阶剪切变形理论(FSDT)、高阶剪切变形理论(HSDT)、准三维剪切变形理论(quasi-3D)和三维弹性理论[12-13]。由于计算成本高和结构特性上的不吻合,三维弹性理论较少地被使用。二维板理论中,CPT由于忽略了剪切效应而仅对薄板提供可接受的分析结果。FSDT考虑了剪切效应,同时将CPT的C^1连续性要求降低到C^0连续性要求,然而FSDT需要利用剪切校正因子(SCF)来校正剪切应变分量,确定剪切校正因子则十分复杂。HSDT具有考虑剪切变形,以及不用计算剪切因子的特性,然而大多数HSDTs忽略了厚向拉伸效应对响应的影响,Carrera等[14]论证了厚向拉伸效应对功能梯度(FGM)板壳响应分析的重要性,其通过多组对比发现,厚向拉伸效应在功能梯度中厚板壳和厚板壳的计算中至关重要,他们还发现,对于夹芯板壳,即便是薄板的情况也必须考虑厚向拉伸效应。

考虑厚度拉伸效应的准三维理论相继被提出,Carrera等[14]提出了Carrera统一公式(CUF),CUF将所有位移分量用泰勒级数展开,通过不同的截断数使得其能够分层细化以接近任何级别的精度。Zenkour[15]利用正弦函数发展了功能梯度板的准三维理论。Matsunaga[16-17]将面内和横向位移利用幂级数展开构造了准三维理论。Neves等[18-20]提出了混合多项式和非多项式的准三维剪切变形理论,面内位移利用非多项式位移场展开,面外位移利用多项式位移场展开,以此构造了多种准三维剪切变形理论。Mantari等[21]提出了一般公式,可以利用多项式、混合或三角函数推导多种准三维理论,还优化了基于tangential的准三维剪切变形理论的未知数个数[22]。Thai等[23]利用sinusodial构造了一种5个未知数的准三维剪切变形理论,主要思路是将横向位移分为弯曲、剪切、厚度影响3个部分,采用类似思路的还有Thai等[24]、Hebali等[25]、Bessaim等[26]、Bennoun等[27]构造的准三维剪切理论。黎梦真[28]提出了一种统一模型,根据横向位移和横向剪应变的类型,可以方便地对各种位移场进行分类。准三维理论是高阶剪切变形理论的一种修正,基于此得到的响应分析结果通常比高阶剪切变形理论更准确。

利用准三维剪切变形理论对带复杂切口功能梯度板自由振动分析的研究十分有限,Van Do等[29]利用只包含4个未知量的简化准三维理论研究了数种带有复杂切口功能梯度板的自由振动。Huang等[30]利用三维弹性理论研究了不同边界条件下带有圆孔的矩形板的自由振动。Yin等[31]利用水平集(level sets)的方法处理等几何图形上的切口,分析了复合材料薄板的振动和屈曲。Tran等[32]利用6个变量的准三维理论、Thai等[33]利用4个未知变量的准三维理论、Nguyen等[10]利用三维弹性理论、Zang等[34]利用等几何尺度边界有限元法分析了带有心型切口的功能梯度板的自由振动。钟锐等[35]利用一阶剪切变形理论等几何方法对功能梯度开孔平行四边形板进行了自由振动分析。对复杂切口的描述不精确,以及采用精度不够的准三维剪切变形理论常常影响到振动分析的精度。

本研究提出一种新的基于准三维剪切变形理论的等几何高精度方法来分析具有复杂切口的FGM板的自由振动。该准三维变形理论称为谱位移格式(SDF),其将未知位移场利用Chebyshev多项式展开,和CUF一样,具有层级细化能力,能使分析结果和三维基准解完美吻合,相较于很多准三维理论,其精度得到进一步提高。同时,其是CPT的拓展,可以避免CUF遇到的剪切闭锁问题,因此对薄板、厚板都具有很好的通用性[36-37]。

1　谱位移格式和控制方程离散

1.1　功能梯度板

考虑如图1所示的功能梯度(FGM)板,其中面位于oxy平面中,厚度为h。假定FGM板由陶瓷和

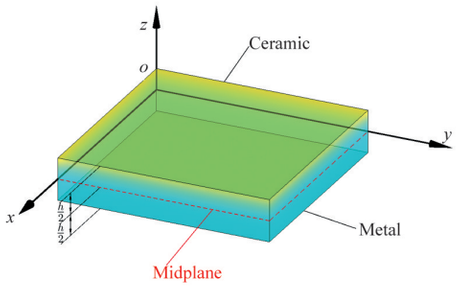

图1 功能梯度板

金属在厚度方向按如下幂律混合制成[13]。

$$\begin{aligned} v_c &= (1/2 + z/h)^g \\ v_m &= 1 - v_c, \qquad z \in [-h/2, h/2] \end{aligned} \tag{1}$$

其中v_c和v_m分别为陶瓷和金属的体积分数,g为梯度指数[13]。

由混合定律,FGM板中各处的等效材料属性可表示为[13]

$$(E,\nu,\rho) = (E_c,\nu_c,\rho_c)v_c + (E_m,\nu_m,\rho_m)v_m \tag{2}$$

其中E、ν和ρ分别为等效弹性模量、泊松比和质量密度,E_c、ν_c和ρ_c及E_m、ν_m和ρ_m分别为陶瓷和金属的相应材料属性。

1.2 谱位移格式和积分控制方程

采用第1类Chebyshev多项式作为谱基底[37],将FGM板的位移场在厚度方向展开为如下谱级数形式

$$\boldsymbol{u} = \boldsymbol{u}_0 + \sum_{i=1}^{M} \boldsymbol{A}_i(z)\boldsymbol{u}_i + \sum_{i=M+1}^{N} \boldsymbol{A}_i(z)\boldsymbol{u}_i \tag{3}$$

其中$\boldsymbol{u}_i$为广义位移,M和N分别为横向和面内位移展开截断数,$M \leqslant N$;且

$$\begin{aligned} &\boldsymbol{u}_0 = [u_0,v_0,0]^{\mathrm{T}},\ \boldsymbol{A}_i(z) = \mathrm{diag}[k_i(z),k_i(z),k_i'(z)] \\ &\boldsymbol{u}_i = \begin{cases} [u_i - w_{i-1,x}, v_i - w_{i-1,y}, w_{i-1}]^{\mathrm{T}}, & 1 \leqslant i \leqslant M \\ [u_i, v_i, 0]^{\mathrm{T}}, & (M+1) \leqslant i \leqslant N \end{cases} \end{aligned} \tag{4}$$

其中,$\{u_i\}_{i=0}^{N}$、$\{v_i\}_{i=0}^{N}$和$\{w_i\}_{i=0}^{M-1}$为广义位移分量,仅为面内坐标(x,y)的函数,$\{k_i(z)\}_{i=1}^{N}$是省略了常数项的谱基底,$(\,)'$表示求一阶导数,$k_i'(z)$为放缩的第2类Chebyshev多项式,$(\,)_{,x}$和$(\,)_{,y}$则分别表示对面内坐标x和y求偏导。相应无限小应变场[38]可写为

$$\boldsymbol{\varepsilon} = \boldsymbol{\varepsilon}_0 + \sum_{i=1}^{M} \boldsymbol{B}_i(z)\boldsymbol{\varepsilon}_i + \sum_{i=M+1}^{N} \boldsymbol{B}_i(z)\boldsymbol{\varepsilon}_i \tag{5}$$

其中,$\boldsymbol{\varepsilon}=[\varepsilon_{xx},\varepsilon_{yy},\varepsilon_{zz},\gamma_{yz},\gamma_{xz},\gamma_{xy}]^{\mathrm{T}}$,$\boldsymbol{\varepsilon}_i$为广义应变,且

$$\begin{aligned} &\boldsymbol{\varepsilon}_0 = [u_{0,x},\nu_{0,y},0,0,0,u_{0,y} + \nu_{0,x}]^{\mathrm{T}} \\ &\boldsymbol{B}_i(z) = \mathrm{diag}[k_i(z),k_i(z),k_i''(z),k_i'(z),k_i'(z),k_i(z)] \\ &\boldsymbol{\varepsilon}_i = \begin{cases} [u_{i,x} - w_{i-1,xx}, \nu_{i,y} - w_{i-1,yy}, w_{i-1}, \nu_i, u_i, u_{i,y} \\ \quad + \nu_{i,x} - 2w_{i-1,xy}]^{\mathrm{T}}, & 1 \leqslant i \leqslant M \\ [u_{i,x}, u_{i,y}, 0, \nu_i, u_i, u_{i,y} + \nu_{i,x}]^{\mathrm{T}}, & (M+1) \leqslant i \leqslant N \end{cases} \end{aligned} \tag{6}$$

$(\,)''$表示求二阶导数。考虑完整的三维弹性本构[38],由Hooke定律,应力场可表示为

$$\begin{aligned} &\boldsymbol{\sigma} = \boldsymbol{D}\boldsymbol{\varepsilon} = \boldsymbol{D}\boldsymbol{\varepsilon}_0 + \sum_{i=1}^{M} \boldsymbol{D}\boldsymbol{B}_i(z)\boldsymbol{\varepsilon}_i + \sum_{i=M+1}^{N} \boldsymbol{D}\boldsymbol{B}_i(z)\boldsymbol{\varepsilon}_i \\ &\boldsymbol{D} = \begin{bmatrix} \boldsymbol{D}_n & 0_{3\times3} \\ 0_{3\times3} & \boldsymbol{D}_s \end{bmatrix}, (\boldsymbol{D}_n)_{ij} = \lambda + 2\mu\delta_{ij}, (\boldsymbol{D}_s) = \mu\delta_{ij} \end{aligned} \tag{7}$$

其中,$\boldsymbol{\sigma}=[\sigma_{xx},\sigma_{yy},\sigma_{zz},\sigma_{yz},\sigma_{xz},\sigma_{xy}]^{\mathrm{T}}$,$\lambda=E\nu/(1+\nu)/(1-2\nu)$和$\mu=E/(1+\nu)/2$为Lamé参数,$\delta_{ij}$为Kronecker符号。

FGM板自由振动的积分控制方程可写为

$$\int_{\nu} \delta\boldsymbol{\varepsilon}^{\mathrm{T}}\boldsymbol{\sigma}\mathrm{d}\nu = \int_{\nu} \delta\mathbf{u}^{\mathrm{T}}(-\rho\ddot{\boldsymbol{u}})\mathrm{d}\nu \tag{8}$$

结合式(3)~式(7),式(8)可整理为二维格式

$$\int_{\Omega} \delta\tilde{\boldsymbol{\varepsilon}}^{\mathrm{T}}\tilde{\boldsymbol{D}}\tilde{\boldsymbol{\varepsilon}}\mathrm{d}a = \omega^2 \int_{\Omega} \delta\tilde{\boldsymbol{u}}^{\mathrm{T}}\boldsymbol{\Lambda}\tilde{\boldsymbol{u}}\mathrm{d}a \tag{9}$$

其中,$\tilde{\boldsymbol{D}}$和$\boldsymbol{\Lambda}$分别为模量阵和惯量阵,ω为简谐振

$$\tilde{\boldsymbol{u}} = \begin{Bmatrix} \boldsymbol{u}_0 \\ \vdots \\ \boldsymbol{u}_N \end{Bmatrix},\ \tilde{\boldsymbol{\varepsilon}} = \begin{Bmatrix} \boldsymbol{\varepsilon}_0 \\ \vdots \\ \boldsymbol{\varepsilon}_N \end{Bmatrix},\ \boldsymbol{\Lambda} = \begin{bmatrix} \boldsymbol{\Lambda}_{00} & \cdots & \boldsymbol{\Lambda}_{0N} \\ \vdots & \ddots & \vdots \\ \boldsymbol{\Lambda}_{0N} & \cdots & \boldsymbol{\Lambda}_{NN} \end{bmatrix},$$

$$\tilde{\boldsymbol{D}} = \begin{bmatrix} \tilde{\boldsymbol{D}}_{00} & \cdots & \tilde{\boldsymbol{D}}_{0N} \\ \vdots & \ddots & \vdots \\ \tilde{\boldsymbol{D}}_{0N} & \cdots & \tilde{\boldsymbol{D}}_{NN} \end{bmatrix}$$

$$\begin{aligned} &(\boldsymbol{\Lambda}_{00},\boldsymbol{\Lambda}_{0j},\boldsymbol{\Lambda}_{ij}) = \int_{-h/2}^{h/2} (\boldsymbol{I}_{3\times3}, \boldsymbol{A}_j(z), \\ &\boldsymbol{A}_i(z)\boldsymbol{A}_j(z))\mathrm{d}z,\ 1 \leqslant i,j \leqslant N \\ &(\tilde{\boldsymbol{D}}_{00},\tilde{\boldsymbol{D}}_{0j},\tilde{\boldsymbol{D}}_{ij}) = \\ &\int_{-h/2}^{h/2} (\boldsymbol{D}, \boldsymbol{D}\boldsymbol{B}_j(z), \boldsymbol{B}_i(z)\boldsymbol{D}\boldsymbol{B}_j(z))\mathrm{d}z,\ 1 \leqslant i,j \leqslant N \\ &\begin{cases} \boldsymbol{\Lambda}_{ji} = (\boldsymbol{\Lambda}_{ij})^{\mathrm{T}} \\ \tilde{\boldsymbol{D}}_{ji} = (\tilde{\boldsymbol{D}}_{ij})^{\mathrm{T}} \end{cases} \forall i,j \in [0,N] \end{aligned} \tag{10}$$

1.3 等几何离散

上述位移场中包含作为广义位移的偏导数,数值分析中应至少采用C^1连续的离散化基底,等几

何分析方法能够满足任意阶次的连续性要求,本文采用等几何分析中的NURBS基底对积分控制方程进行离散。

给定由二维NURBS基底表示的FGM板中面几何模型[37-40]

$$\Omega=\left\{\boldsymbol{x}=(x,y)\,\middle|\,\boldsymbol{x}(\zeta)=\sum_{\lceil\mathbf{i}\rceil=1}^{Q}\boldsymbol{x}_{\lceil\mathbf{i}\rceil}R_{\lceil\mathbf{i}\rceil}(\zeta),\zeta=(\zeta,\eta)\in\widehat{\Omega}\right\} \tag{11}$$

其中,$\lceil\mathbf{i}\rceil$为字典序,$\boldsymbol{x}_{\lceil\mathbf{i}\rceil}$为几何控制点,$\widehat{\Omega}$为板中面$\Omega$在二维参数空间中的映射。$R_{\lceil\mathbf{i}\rceil}$为二维NURBS基底,将其继续用于位移场面内离散可得

$$\boldsymbol{q}(\zeta)=\sum_{\lceil\mathbf{i}\rceil=1}^{Q}\boldsymbol{q}_{\lceil\mathbf{i}\rceil}R_{\lceil\mathbf{i}\rceil}(\zeta) \tag{12}$$

其中,$\boldsymbol{q}=[u_0,\cdots,u_N,v_0,\cdots,v_N,w_0,\cdots,w_{M-1}]^{\mathrm{T}}$为板位移场的基本未知场,$\boldsymbol{q}_{\lceil\mathbf{i}\rceil}$为控制向量,且

$$\begin{aligned}\tilde{\boldsymbol{u}}(\zeta)&=\sum_{\lceil\mathbf{i}\rceil=1}^{Q}\boldsymbol{U}_{\lceil\mathbf{i}\rceil}(\zeta)\boldsymbol{q}_{\lceil\mathbf{i}\rceil}\\\tilde{\boldsymbol{\varepsilon}}(\zeta)&=\sum_{\lceil\mathbf{i}\rceil=1}^{Q}\boldsymbol{E}_{\lceil\mathbf{i}\rceil}(\zeta)\boldsymbol{q}_{\lceil\mathbf{i}\rceil}\end{aligned} \tag{13}$$

其中,$\boldsymbol{U}_{\lceil\mathbf{i}\rceil}$和$\boldsymbol{E}_{\lceil\mathbf{i}\rceil}$均为稀疏矩阵,元素表达式可见Yang等相关文章[37]。

将式(13)代入式(9)并整理,可得FGM板自由振动分析的离散化控制方程

$$\begin{aligned}&\sum_{\lceil\mathbf{j}\rceil=1}^{Q}\boldsymbol{K}_{\lceil\mathbf{i}\rceil\lceil\mathbf{j}\rceil}\boldsymbol{q}_{\lceil\mathbf{j}\rceil}=\omega^2\sum_{\lceil\mathbf{j}\rceil=1}^{Q}\boldsymbol{M}_{\lceil\mathbf{i}\rceil\lceil\mathbf{j}\rceil}\boldsymbol{q}_{\lceil\mathbf{j}\rceil},\\&\forall\lceil\mathbf{i}\rceil\in[1,Q]\quad\boldsymbol{M}_{\lceil\mathbf{i}\rceil\lceil\mathbf{j}\rceil}=\int_{\widehat{\Omega}}\boldsymbol{U}_{\lceil\mathbf{i}\rceil}^{\mathrm{T}}\Lambda\boldsymbol{U}_{\lceil\mathbf{j}\rceil}J_a\,\mathrm{d}\,\widehat{a}\end{aligned} \tag{14}$$

其中,$\boldsymbol{M}_{\lceil\mathbf{i}\rceil\lceil\mathbf{j}\rceil}$为块一致质量阵。

式(14)可进一步写为整体形式,即

$$\boldsymbol{K}\boldsymbol{d}=\omega^2\boldsymbol{M}\boldsymbol{d} \tag{15}$$

其中,整体矩阵和向量,即刚度阵$\boldsymbol{K}$、质量阵$\boldsymbol{M}$、基本未知控制向量$\boldsymbol{d}$分别由$\boldsymbol{K}_{\lceil\mathbf{i}\rceil\lceil\mathbf{j}\rceil}$、$\boldsymbol{M}_{\lceil\mathbf{i}\rceil\lceil\mathbf{j}\rceil}$、$\boldsymbol{q}_{\lceil\mathbf{j}\rceil}$依照既定标量字典序[41],通过简单的逐块组装过程得到。

NURBS基底的局部支撑性将保证结构矩阵$\boldsymbol{K}$和$\boldsymbol{M}$的稀疏性[39]。

2　数值结果和讨论

为验证本研究所提出基于谱位移格式的等几何分析方法在带复杂切口功能梯度板自由振动分析中的准确性和通用性,对3种带复杂切口形状的功能梯度板进行了自由振动分析,所有算例中,均采用4阶NURBS基底,面内单元内采用$(p+1)(q+1)$全高斯积分点策略[39],厚度方向的积分点数依赖于梯度指数值,由被积函数的多项式阶数确定,见式(10)。由于NURBS基函数一般不具有插值特性,利用罚方法施加边界条件和片耦合[42-43],根据数值试验,边界条件罚系数取相关单元刚度阵最大元素值的10^4倍,SDF截断数选取M=5,N=6。算例中涉及的组分材料属性列于表1。代码由MATLAB 9.10编译,运行在Intel(R) Core (TM) i7-9750H CPU (2.60GHz),Win10 64位操作系统,32GB RAM 12线程的计算机上。

表1　陶瓷和金属材料属性

材料类型	杨氏模量E/GPa	泊松比ν	密度ρ/(kg·m^{-3})
Al	70	0.3	2702
ZrO_2	270	0.3	5700

2.1　四花瓣型切口方板

考虑具有对称性的四花瓣型切口Al/ZrO_2方板,等几何模型如图2所示。该模型由8个NURBS片组成,构成网格的结点线由红色实线表示,控制点以蓝色实心点表示。材料属性如表1所示。为便于观察和比较,定义以下无量纲响应$\bar{\omega}=\omega L^2\sqrt{\rho_c/E_c}/h$,其中$L$是方板边长,$h$为方板厚度。

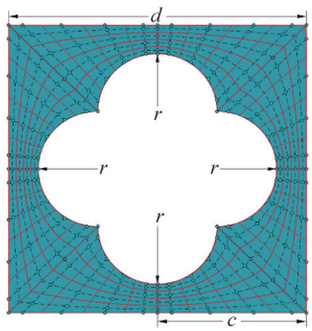

d=10, c=5, r=2

图2　四花瓣型切口方板的NURBS中面模型

当厚度h=0.5时,表2、表3列出了四花瓣型切口方板在不同梯度指数下的无量纲自然频率结果,并与基于简化准三维理论的等几何结果[29]进行了对比,可以看出,结果与参考解符合得很好,考虑到

表2 Al/ZrO_2四花瓣型切口方孔板简支边界下的自振无量纲频率

模型	方法	g=0.5	g=1	g=5	g=10	g=100
1	Quasi-3D IGA[29]	9.1810	8.9700	9.1430	9.1210	8.5360
	Present	9.2237	8.9712	9.1462	9.1252	8.5385
2	Quasi-3D IGA[29]	11.4340	11.2260	10.5920	10.3800	10.1100
	Present	11.3248	11.2260	10.5926	10.3813	10.1104
3	Quasi-3D IGA[29]	12.0950	11.8170	11.9760	11.9410	11.2160
	Present	12.1483	11.8174	11.9782	11.9445	11.2188
4	Quasi-3D IGA[29]	12.0960	11.8170	11.9760	11.9410	11.2170
	Present	12.1483	11.8174	11.9782	11.9445	11.2188
5	Quasi-3D IGA[29]	15.4490	15.0930	15.2280	15.1760	14.2970
	Present	15.5151	15.0930	15.2291	15.1802	14.3002
6	Quasi-3D IGA[29]	31.1750	30.4550	29.7480	29.1550	28.3960
	Present	31.3071	30.4747	29.7487	29.1559	28.3955
7	Quasi-3D IGA[29]	32.1130	31.5280	29.7490	29.1550	28.3960
	Present	31.7984	31.5279	29.7487	29.1559	28.3955
8	Quasi-3D IGA[29]	32.1130	31.5280	30.8000	30.7040	28.8790
	Present	31.7984	31.5279	30.8208	30.7292	28.9036
9	Quasi-3D IGA[29]	36.6720	35.8250	36.1210	35.9960	33.9250
	Present	36.8398	35.8549	36.1513	36.0342	33.9612
10	Quasi-3D IGA[29]	36.6730	35.8250	36.1210	35.9960	33.9250
	Present	36.8398	35.8549	36.1513	36.0342	33.9612

表3 Al/ZrO_2四花瓣型切口方孔板固支边界下的自振无量纲频率

模型	方法	g=0.5	g=1	g=5	g=10	g=100
1	Quasi-3D IGA[29]	25.3510	24.7640	24.9170	24.8220	23.4330
	Present	25.5210	24.8262	24.9864	24.8980	23.4939
2	Quasi-3D IGA[29]	25.4250	24.8360	24.9810	24.8870	23.4950
	Present	25.5943	24.8985	25.0449	24.9551	23.5563
3	Quasi-3D IGA[29]	25.4370	24.8490	25.0050	24.9130	23.5120
	Present	25.5943	24.8985	25.0449	24.9551	23.5563
4	Quasi-3D IGA[29]	25.5110	24.9220	25.0590	24.9650	23.5720
	Present	25.6685	24.9718	25.1041	25.0129	23.6194
5	Quasi-3D IGA[29]	58.3280	56.9700	56.7990	56.5350	53.6885
	Present	58.6841	57.1435	56.9669	56.7166	53.8532
6	Quasi-3D IGA[29]	59.3040	57.9200	57.6890	57.4160	54.5540
	Present	59.6692	58.1055	57.8851	57.6283	54.7430
7	Quasi-3D IGA[29]	59.3620	57.9850	57.8070	57.5430	54.6360
	Present	59.6692	58.1055	57.8851	57.6283	54.7430
8	Quasi-3D IGA[29]	60.5200	59.1120	58.8590	58.5830	55.6670
	Present	60.8314	59.2403	58.9689	58.7048	55.7932
9	Quasi-3D IGA[29]	74.3300	72.5850	71.8300	71.4420	68.1730
	Present	74.6406	72.7272	72.0209	71.6679	68.3420
10	Quasi-3D IGA[29]	74.6470	72.8980	72.1810	71.8050	68.4760
	Present	74.9656	73.0464	72.3125	71.9566	68.6322

结构的对称性,本研究给出的计算结果更加合理。例如,在固支边界条件下,当g=0.5,本研究方法计算的固有频率结果体现出了结构的对称性。从表2中还可以看出,梯度指数会明显改变结构固有频率,尤其会改变同频固有频率出现的阶次,例如,在简支边界条件下,g=0.5时,7阶和8阶固有频率相等,g=5时,6阶和7阶固有频率相等。

图3、图4展示了当g=1时,简支边界条件和固支边界条件下板相应的前6阶自振模态(h/L=0.05)。通过图3、图4可以看出边界条件影响了前6阶振型形状。

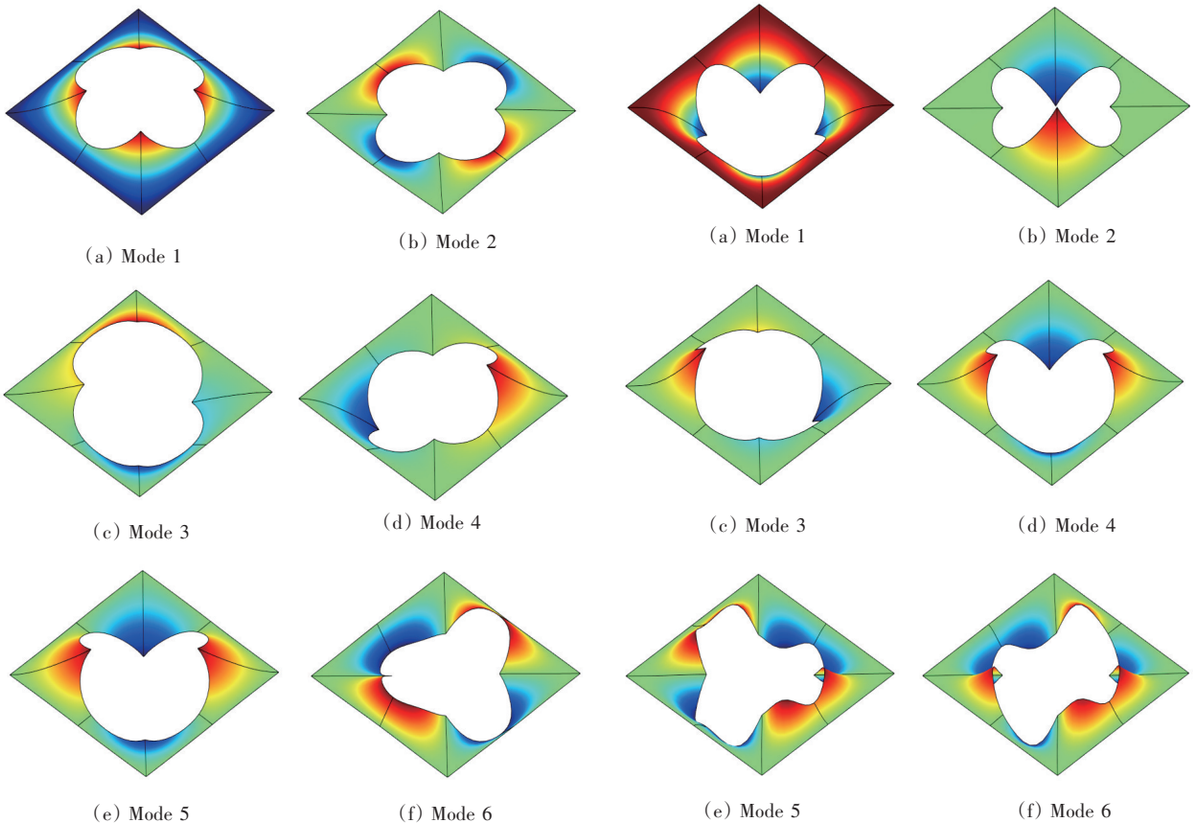

图3　简支边界下,Al/ZrO_2四花瓣型切口方板前6阶振动模态

图4　固支边界下,Al/ZrO_2四花瓣型切口方板前6阶振动模态

2.2　三花瓣型切口方板

考虑具有对称性的三花瓣型切口Al/ZrO_2方板,等几何模型如图5所示,其中d=10,c=4,r=2。该模型有9个NURBS片组成,定义以下无量纲响应$\overline{\omega} = \omega L^2 \sqrt{\rho_c / E_c} / h$

当厚度h=0.5时,表4、表5列出了三花瓣型切口方板在不同梯度指数下的无量纲自然频率结果,并与基于简化准三维理论的等几何结果[29]进行了对比,可以看出,本研究结果与参考解符合得很好。从表中可以看到,相较于简支边界条件,固支边界条件下自振频率变大。另外,梯度指数对固有频率影响较小。

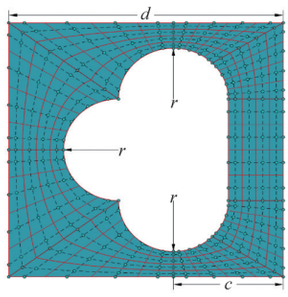

图5　三花瓣型切口方板的NURBS中面模型

表4 Al/ZrO_2三花瓣型切口方孔板简支边界下的自振无量纲频率

模型	方法	g=0.5	g=1	g=5	g=10	g=100
1	Quasi-3D IGA[29]	7.4410	7.2690	7.4060	7.3880	6.9160
	Present	7.4307	7.2260	7.3632	7.3459	6.8760
2	Quasi-3D IGA[29]	10.7700	10.5220	10.6640	10.6330	9.9880
	Present	10.8206	10.5264	10.6694	10.6394	9.9931
3	Quasi-3D IGA[29]	12.0970	11.8180	11.9680	11.9310	11.2140
	Present	12.1262	11.7941	11.9455	11.9111	11.1932
4	Quasi-3D IGA[29]	17.0780	16.7670	15.8200	15.5040	15.1010
	Present	16.9645	16.8168	15.8680	15.5515	15.1455
5	Quasi-3D IGA[29]	20.2810	19.8130	20.0630	20.0010	18.8000
	Present	20.4598	19.9039	20.1606	20.1033	18.8911
6	Quasi-3D IGA[29]	24.6430	24.0750	24.3440	24.2670	22.8280
	Present	24.7128	24.0420	24.3180	24.2458	22.8045
7	Quasi-3D IGA[29]	31.2920	30.7210	28.9890	28.4100	27.6700
	Present	31.1245	30.8590	29.1197	28.5390	27.7941
8	Quasi-3D IGA[29]	31.8660	31.1320	31.3720	31.2600	29.4740
	Present	32.1359	31.2625	31.5149	31.4127	29.6095
9	Quasi-3D IGA[29]	33.4820	32.7080	33.0270	32.9190	30.9970
	Present	33.4461	32.5473	32.8656	32.7653	30.8528
10	Quasi-3D IGA[29]	38.7940	38.0880	35.9400	35.2220	34.3020
	Present	38.5162	38.1790	36.0262	35.3073	34.3844

表5 Al/ZrO_2三花瓣型切口方孔板固支边界下的自振无量纲频率

模型	方法	g=0.5	g=1	g=5	g=10	g=100
1	Quasi-3D IGA[29]	18.3520	17.9290	18.1310	18.0740	17.0030
	Present	18.3257	17.8212	18.0183	17.9621	16.8991
2	Quasi-3D IGA[29]	20.7680	20.2890	20.4440	20.3720	19.2090
	Present	20.8216	20.2524	20.4035	20.3338	19.1743
3	Quasi-3D IGA[29]	27.5190	26.8830	27.0910	26.9960	25.4540
	Present	27.7334	26.9801	27.1716	27.0765	25.5394
4	Quasi-3D IGA[29]	35.9300	35.0990	35.2120	35.0720	33.1660
	Present	36.2596	35.2860	35.3779	35.2412	33.3373
5	Quasi-3D IGA[29]	37.2880	36.4260	36.5080	36.3600	34.4050
	Present	37.4559	36.4499	36.5246	36.3832	34.4308
6	Quasi-3D IGA[29]	46.2000	45.1300	45.1640	44.9740	42.5970
	Present	46.1927	44.9582	44.9740	44.7948	42.4382
7	Quasi-3D IGA[29]	47.3520	46.2550	46.2240	46.0230	43.6310
	Present	47.7286	46.4575	46.4017	46.2078	43.8197
8	Quasi-3D IGA[29]	54.5660	53.3000	53.2040	52.9680	50.2520
	Present	54.5977	53.1510	53.0313	52.8087	50.1152
9	Quasi-3D IGA[29]	61.6020	60.1700	59.8910	59.6080	56.6560
	Present	61.4117	59.8036	59.4913	59.2257	56.3129
10	Quasi-3D IGA[29]	62.8010	61.3430	61.0160	60.7220	57.7410
	Present	63.0656	61.4071	61.0484	60.7690	57.8024

图6、图7展示了当g=1时,不同边界条件下板　　出,边界条件对该板振型影响明显。对应的前6阶自振模态(h/L=0.05)。从图中可以看

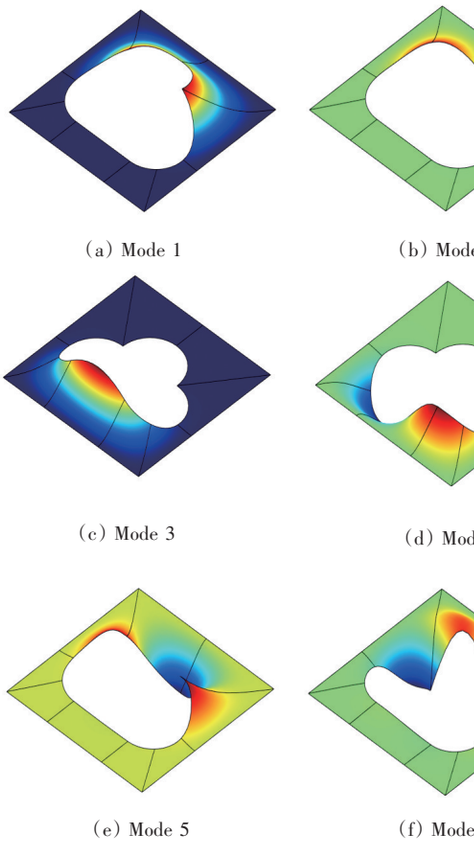

图6　简支边界下,Al/ZrO_2三花瓣型切口方板前6阶振动模态

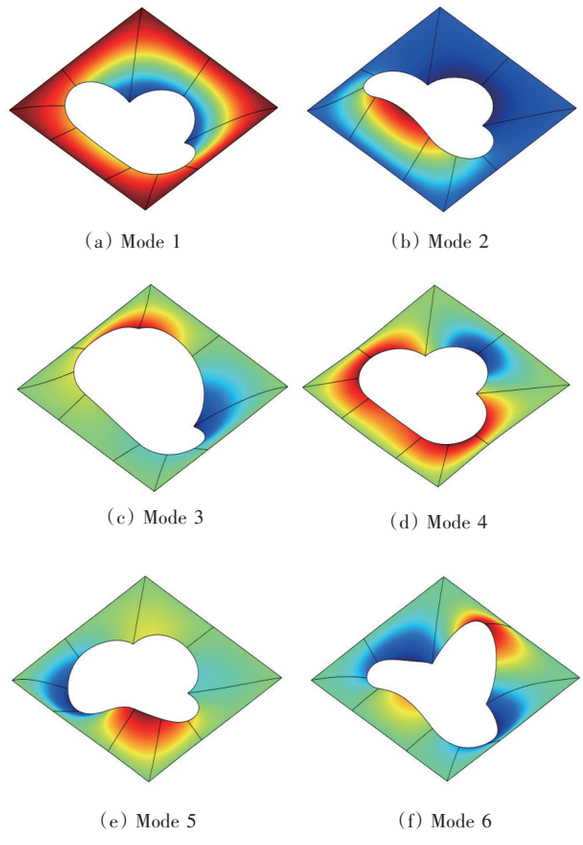

图7　固支边界下,Al/ZrO_2三花瓣型切口方板前6阶振动模态

2.3　四花瓣型切口圆板

考虑具有对称性的四花瓣型切口Al/ZrO_2圆板,等几何模型如图8所示,其中d=10,r=2。该模型有8个NURBS片组成,为便于观察和比较,定义以下无量纲响应$\overline{\omega}=\omega D^2\sqrt{\rho_c/E_c}/h$,其中$D$为圆板的直径,$h$为圆板厚度。

表6列出了固支边界的四花瓣型孔圆板在不同梯度指数和厚度下的无量纲基频结果,并与基于简化准三维理论的等几何结果[29]进行了对比,可以看出,本研究结果与参考解非常吻合。随着板厚度的增加,该板的基础频率显著下降。而梯度指数对基础频率的影响不太明显。

当厚度h=0.5时,表7、表8给出了基于本研究提出方法得到的不同梯度指数下前10阶的自振无量纲频率,本研究结果体现出了板的对称特性,可作为后续分析的基准解。可以看出,边界条件的改变对自振频率的影响巨大。

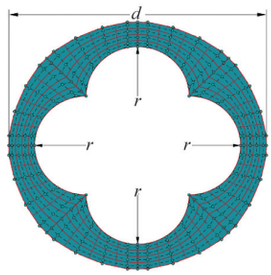

图8　四花瓣型切口圆板的NURBS中面模型

图9、图10展示了当g=1时,不同边界条件下相应的前6阶自振模态(h/D=0.05)。可以看出,边界条件的改变使得该结构的振型发生显著变化。

表6 Al/ZrO_2四花瓣型切口圆孔板固支边界下的无量纲基频

h/D	方法	g=0.5	g=1	g=5	g=10	g=100
0.02	Quasi-3D IGA[29]	43.0932	42.1749	42.8777	42.7067	39.9654
	Present	43.5820	42.3645	43.0986	42.9882	40.2803
0.04	Quasi-3D IGA[29]	41.0441	40.1587	40.4377	40.2549	37.9092
	Present	41.5819	40.4528	40.7805	40.6414	38.3069
0.08	Quasi-3D IGA[29]	35.9988	35.2061	34.7164	34.5229	32.9550
	Present	36.4731	35.5514	35.0823	34.8879	33.3399
0.1	Quasi-3D IGA[29]	33.5662	32.8209	32.0726	31.8823	30.6137
	Present	33.9088	33.0822	32.3394	32.1271	30.8883
0.2	Quasi-3D IGA[29]	24.2619	23.7186	22.5266	22.3712	21.8791
	Present	23.8424	23.3369	22.1356	21.8991	21.4598
0.3	Quasi-3D IGA[29]	18.6473	18.2425	17.1256	16.9975	16.7447
	Present	17.8210	17.4778	16.3621	16.1415	15.9446

表7 Al/ZrO_2四花瓣型切口圆孔板固支边界下的自振无量纲频率

模型	g=0.5	g=1	g=5	g=10	g=100
1	40.3737	39.2968	39.4069	39.2526	37.1238
2	40.4340	39.3563	39.4557	39.3003	37.1753
3	40.4340	39.3563	39.4557	39.3003	37.1753
4	40.4950	39.4163	39.5049	39.3485	37.2274
5	77.4748	75.4983	74.8898	74.5192	70.9793
6	78.8658	76.8588	76.1779	75.7972	72.2335
7	78.8658	76.8588	76.1779	75.7972	72.2335
8	80.7403	78.6926	77.9136	77.5201	73.9248
9	94.8802	92.4931	91.1684	90.6563	86.6973
10	99.8410	97.3418	95.8001	95.2539	91.1839

表8 Al/ZrO_2三花瓣型切口方孔板简支边界下的自振无量纲频率

模型	g=0.5	g=1	g=5	g=10	g=100
1	7.7114	7.5023	7.6419	7.6236	7.1372
2	12.8022	12.4610	12.5663	12.5253	11.8030
3	12.8022	12.4610	12.5663	12.5253	11.8030
4	18.2521	17.7781	17.8242	17.7589	16.7998
5	21.8564	21.6448	20.4293	20.0202	19.4942
6	23.1504	22.9532	21.6573	21.2277	20.6772
7	25.1830	24.9611	23.5537	23.0849	22.4836
8	25.1830	24.9611	23.5537	23.0849	22.4836
9	34.0262	33.1252	33.4170	32.7498	31.3830
10	35.7363	35.4135	33.4297	32.9922	31.8943

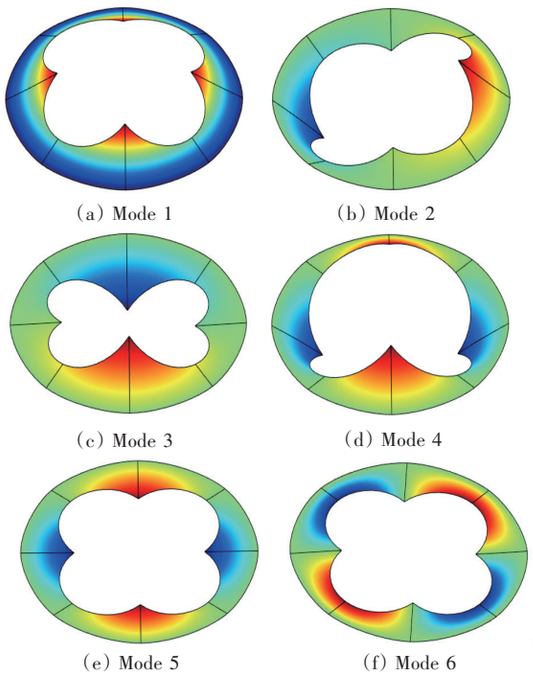

图9 简支边界下Al/ZrO_2四花瓣型切口圆板前6阶振动模态

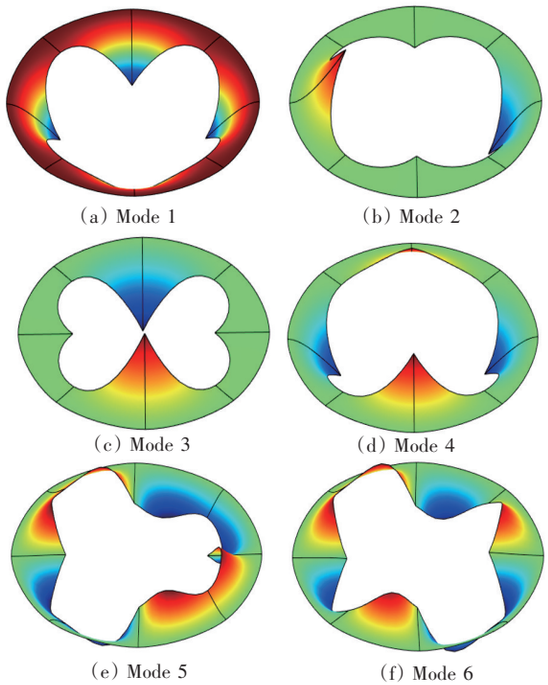

图10 固支边界下Al/ZrO_2四花瓣型切口圆板前6阶振动模态

3　结论

在1阶剪切变形理论中,中面挠度和旋转角度作为各自独立的自由度,当板变的极薄时,场不一致性会导致剪切闭锁现象发生,而经典板理论未采用这种基本设定,能够自然地避免剪切闭锁问题。谱位移格式是经典板理论的拓展,也继承了经典板理论避免剪切闭锁问题的优点。三维弹性本构方程的使用使得谱位移格式考虑了厚向拉伸效应,结合Chebyshev多项式能用较小截断数高精度近似目标函数的谱收敛特性,保证了该剪切变形理论的高精度特性。同时等几何方法能够精确地描述复杂几何,减小离散误差,这使得本方法的精度得到进一步保证。通过数值算例结果可得到以下结论。

1)基于谱位移格式的等几何方法在计算带有复杂切口功能梯度板时具有有效性和通用性。当复杂切口有对称性时,本文方法所得结果能呈现明显的对称特征,反映出计算结果的准确性。

2)厚度变化、边界条件改变对带复杂切口功能梯度板的自由振动模态有显著影响,梯度指数改变也会影响带有复杂切口功能梯度板的自振频率,同时会影响相同固有频率出现的阶次。

通过讨论,证明本研究提出的方法的准确性,其具有分析非线性振动、强迫振动的潜力。后续还可以开展减少未知量个数,以及进一步提升计算效率方面的研究。

参考文献(References)

[1] Xu F X, Zhang X, Zhang H. A review on functionally graded structures and materials for energy absorption[J]. Engineering Structures, 2018, 171: 309-325.

[2] Saleh B, Jiang J H, Fathi R, et al. 30 Years of functionally graded materials: An overview of manufacturing methods, applications and future challenges[J]. Composites Part B: Engineering, 2020, 201: 108376.

[3] Guedes Soares C, Shenoi R A. Analysis and design of marine structures[M]. London: CRC Press, 2009.

[4] Sahoo S. Laminated composite stiffened shallow spherical panels with cutouts under free vibration-A finite element approach[J]. Engineering Science and Technology, an International Journal, 2014, 17(4): 247-259.

[5] Ovesy H R, Fazilati J. Buckling and free vibration finite strip analysis of composite plates with cutout based on two different modeling approaches[J]. Composite Structures, 2012, 94(3): 1250-1258.

[6] Natarajan S, Deogekar P S, Manickam G, et al. Hygrothermal effects on the free vibration and buckling of laminated composites with cutouts[J]. Composite Structures, 2014, 108: 848-855.

[7] Fantuzzi N, Tornabene F, Viola E. Four-parameter functionally graded cracked plates of arbitrary shape: A GDQ-FEM solution for free vibrations[J]. Mechanics of Advanced Materials and Structures, 2016, 23(1): 89-107.

[8] Ansari R, Torabi J, Hassani R. A comprehensive study on the free vibration of arbitrary shaped thick functionally graded CNT-reinforced composite plates[J]. Engineering Structures, 2019, 181: 653-669.

[9] Liu G R, Chen X L. A mesh-free method for static and free vibration analyses of thin plates of complicated shape [J]. Journal of Sound and Vibration, 2001, 241(5): 839-855.

[10] Nguyen K D, Nguyen-Xuan H. An isogeometric finite element approach for three-dimensional static and dynamic analysis of functionally graded material plate structures[J]. Composite Structures, 2015, 132: 423-439.

[11] Hughes T J R, Cottrell J A, Bazilevs Y. Isogeometric analysis: CAD, finite elements, NURBS, exact geometry and mesh refinement[J]. Computer Methods in Applied Mechanics and Engineering, 2005, 194(39/40/41): 4135-4195.

[12] Thai H T, Kim S E. A review of theories for the modeling and analysis of functionally graded plates and shells [J]. Composite Structures, 2015, 128: 70-86.

[13] Jha D K, Kant T, Singh R K. A critical review of recent research on functionally graded plates[J]. Composite Structures, 2013, 96: 833-849.

[14] Carrera E, Brischetto S, Cinefra M, et al. Effects of thickness stretching in functionally graded plates and shells[J]. Composites Part B: Engineering, 2011, 42(2): 123-133.

[15] Zenkour A M. Benchmark trigonometric and 3-D elasticity solutions for an exponentially graded thick rectangular plate[J]. Archive of Applied Mechanics, 2007, 77(4): 197-214.

[16] Matsunaga H. Free vibration and stability of functionally graded plates according to a 2-D higher-order deforma-

tion theory[J]. Composite Structures, 2008, 82(4): 499-512.

[17] Matsunaga H. Free vibration and stability of functionally graded shallow shells according to a 2D higher-order deformation theory[J]. Composite Structures, 2008, 84(2): 132-146.

[18] Neves A M A, Ferreira A J M, Carrera E, et al. A quasi-3D hyperbolic shear deformation theory for the static and free vibration analysis of functionally graded plates[J]. Composite Structures, 2012, 94(5): 1814-1825.

[19] Neves A M A, Ferreira A J M, Carrera E, et al. Static, free vibration and buckling analysis of isotropic and sandwich functionally graded plates using a quasi-3D higher-order shear deformation theory and a meshless technique[J]. Composites Part B: Engineering, 2013, 44(1): 657-674.

[20] Neves A M A, Ferreira A J M, Carrera E, et al. Buckling analysis of sandwich plates with functionally graded skins using a new quasi-3D hyperbolic sine shear deformation theory and collocation with radial basis functions[J]. ZAMM - Journal of Applied Mathematics and Mechanics, 2012, 92(9): 749-766.

[21] Mantari J L, Guedes Soares C. Generalized hybrid quasi-3D shear deformation theory for the static analysis of advanced composite plates[J]. Composite Structures, 2012, 94(8): 2561-2575.

[22] Mantari J L, Soares C G. A quasi-3D tangential shear deformation theory with four unknowns for functionally graded plates[J]. Acta Mechanica, 2015, 226(3): 625-642.

[23] Thai H T, Kim S E. A simple quasi-3D sinusoidal shear deformation theory for functionally graded plates[J]. Composite Structures, 2013, 99: 172-180.

[24] Thai H T, Vo T P, Bui T Q, et al. A quasi-3D hyperbolic shear deformation theory for functionally graded plates[J]. Acta Mechanica, 2014, 225(3): 951-964.

[25] Hebali H, Tounsi A, Houari M S A, et al. New quasi-3D hyperbolic shear deformation theory for the static and free vibration analysis of functionally graded plates[J]. Journal of Engineering Mechanics, 2014, 140(2): 374-383.

[26] Bessaim A, Houari M S, Tounsi A, et al. A new higher-order shear and normal deformation theory for the static and free vibration analysis of sandwich plates with functionally graded isotropic face sheets[J]. Journal of Sandwich Structures & Materials, 2013, 15(6): 671-703.

[27] Bennoun M, Houari M S A, Tounsi A. A novel five-variable refined plate theory for vibration analysis of functionally graded sandwich plates[J]. Mechanics of Advanced Materials and Structures, 2016, 23(4): 423-431.

[28] 黎梦真. 功能梯度板高阶剪切变形理论建模方法与力学特性研究[D]. 武汉: 武汉理工大学, 2021.

[29] Van Do V N, Lee C H. Free vibration analysis of FGM plates with complex cutouts by using quasi-3D isogeometric approach[J]. International Journal of Mechanical Sciences, 2019, 159: 213-233.

[30] Huang W H, Xue K, Li Q H. Three-dimensional solution for the vibration analysis of functionally graded rectangular plate with/without cutouts subject to general boundary conditions[J]. Materials, 2021, 14(22): 7088.

[31] Yin S H, Yu T T, Bui T Q, et al. A cutout isogeometric analysis for thin laminated composite plates using level sets[J]. Composite Structures, 2015, 127: 152-164.

[32] Tran L V, Abdel Wahab M, Kim S E. An isogeometric finite element approach for thermal bending and buckling analyses of laminated composite plates[J]. Composite Structures, 2017, 179: 35-49.

[33] Thai C H, Zenkour A M, Abdel Wahab M, et al. A simple four-unknown shear and normal deformations theory for functionally graded isotropic and sandwich plates based on isogeometric analysis[J]. Composite Structures, 2016, 139: 77-95.

[34] Zang Q S, Liu J, Ye W B, et al. Static and free vibration analyses of functionally graded plates based on an isogeometric scaled boundary finite element method[J]. Composite Structures, 2022, 288: 115398.

[35] 钟锐, 胡双卫, 秦斌, 等. 功能梯度开孔平行四边形板的等几何振动分析[J]. 哈尔滨工程大学学报, 2022, 43(7): 999-1005.

[36] Sun X B, Gao R X, Zhang Y H. Spectral stochastic isogeometric analysis of bending and free vibration of porous functionally graded plates[J]. Applied Mathematical Modelling, 2023, 116: 711-734.

[37] Yang S W, Sun X B, Cai Z Q, et al. High-precision isogeometric static bending analysis of functionally graded plates using a new quasi-3D spectral displacement formulation[J]. Applied Sciences, 2023, 13(11): 6412.

[38] Szilard R. Theories and applications of plate analysis: Classical, numerical and engineering methods[J]. Applied Mechanics Reviews, 2004, 57(6): B32-B33.

[39] Cottrell J A, Hughes T J R, Bazilevs Y. Isogeometric analysis: Toward integration of CAD and FEA[M]. NJ,

USA: John Wiley & Sons, 2009.
[40] Piegl L, Tiller W. The NURBS book[M]. Berlin, Germany: Springer Science & Business Media, 1996.
[41] Cox D A, Little J, O'Shea D. Ideals, varieties, and algorithms: An introduction to computational algebraic geometry and commutative algebra[M]. Berlin: Springer Cham, 2015.
[42] Babuška I. The finite element method with penalty[J]. Mathematics of Computation, 1973, 27(122): 221-228.
[43] Fernández-Méndez S, Huerta A. Imposing essential boundary conditions in mesh-free methods[J]. Computer Methods in Applied Mechanics and Engineering, 2004, 193(12/13/14): 1257-1275.

Isogeometric analysis for free vibration of functionally graded plates with complex cutouts using spectral displacement formulation

YANG Shaowei[1], SUN Xianbo[1], CAI Zhiqin[1*], LU Hailong[1], YANG Zhixun[2]

1. Department of Engineering Mechanics, Dalian University of Technology, Dalian 116024, China
2. College of Mechanical and Electrical Engineering, Harbin Engineering University, Harbin 150001, China

Abstract This paper aims to analyze the free vibration response of functionally graded plates with complex cutouts. An isogeometric analysis method based on a novel quasi-three-dimensional higher-order shear deformation theory called the spectral displacement formulation (SDF) is employed to predict the free vibration characteristics of the plates. The SDF can deal with the three-dimensional elasticity solution and naturally avoid the shear-locking problem, making it suitable for plates with varying thicknesses. The governing equations for free vibration of the plates are derived using the D'Alembert principle and the principle of virtual work, and the equations are discretized using isogeometric method. The results of several numerical examples are compared with existing reference solutions. It is concluded that the proposed analysis method can accurately and effectively analyze the free vibration of functionally graded plates with complex cutouts.

Keywords functionally graded plate; cutout; spectral displacement formulation; isogeometric analysis; free vibration

（责任编辑　王微）